# Singularities of resistivity and thermoelectric power of metals in phase transitions of order $2^1/_2$

V. G. Vaks, A.V. Trefilov, and S. V. Fomichev

(Submitted 28 October 1980)
Zh. Eksp. Teor. Fiz. **80**, 1613–1621 (April 1981)

It is shown that all the kinetic coefficients of a metal, including the electric resistivity, have singularities of the $z^{1/2}$ type in phase transitions of order 2 1/2, while the thermoelectric power has singularities of the $z^{-1/2}$ type ($z$ is the parameter of the proximity to the transition point). Calculation results are presented and indicate that these effects are appreciable and can be used to observe transitions of order 2 1/2, as well as to investigate the degree of smearing of the Fermi surface in metals.

PACS numbers: 72.15.Eb, 72.15.Jf, 64.60.Fr

## 1. INTRODUCTION

Lifshitz's well known paper[1] on phase transitions of order $2\frac{1}{2}$ due to change of the Fermi-surface (FS) topology contains a remark that the kinetic coefficients of the metal should apparently have in these transitions singularities of the $|z|^{1/2}$ or $|z|^{-1/2}$ type (neglecting the FS temperature smearing that leads to a smoothing of the singularities in a narrow vicinity $|z|\leq T$ of the transition). Here $z=\mu-\mu_c$ ($\mu$ is the chemical potential of the electrons and $\mu_c$ is its critical value) is the parameter of proximity to the transition, and is proportional, for example, to $P-P_c$ if the transition is with respect to the pressure $P$. Further more detailed treatments (see the review by Kaganov and Lifshitz[2]), however, dealt only with singularities of sound absorption and of the acousto-emf, which seem to be quite complicated for quantitative measurements, especially under pressure. Furthermore, no singularities in the electron mean free path $l$ were considered.

We wish to note in this article that, in accord with Lifshitz's original remarks,[1] singularities of type $z^{1/2}\theta(z)$ or $(-z)^{1/2}\theta(-z)$ connected with $l$ [where $\theta(x)$ is zero at $x<0$ and 1 at $x>0$] are observed in all the kinetic coefficients, including the electric and thermal conductivities, while in the thermoelectric power $\alpha$ this singularity strengthens to $(\pm z)^{-1/2}\theta(\pm z)$. Here and elsewhere $\theta(-z)$ corresponds to the region of "tangency" of the FS with a face of the Brillouin zone (BZ), and $\theta(z)$ corresponds to the "overflow" region, of formation of a new cavity. We note that singularities of this type were in fact discussed already by Ziman[3] in his attempt to explain the (later dubbed Kohn) anomalies of the impurity resistivity $\rho$ in Cu. Ziman, however, confined himself to an estimate of $\rho$ in a crude model (that admits of analytic solution) and to its application to Cu, where it was not adequate. Ziman's arguments[3] were not noted in the subsequent general treatments.[1,2]

It is of interest to study transions of order $2\frac{1}{2}$ in alloys. The opinion was advanced that they are not observable there, because the concepts of quasimomentum and FS have not been formally defined for disordered alloys.[4] However, experimental observations of Kohn anomalies in their phonon spectra,[5] as well as theoretical estimates,[6] show that the smearing of the FS is apparently small in many alloys of metals having close properties, although quantitative information on the degree of this smearing is still lacking. It is shown below that this information can be obtained by observing the anomalies of $\rho$ and $\alpha$ in transitions of order $2\frac{1}{2}$ in alloys.

To illustrate the scale of the discussed anomalies, we present results of the calculation of the functions $\rho(x)$ and $\alpha(x)$ in $Li_{1-x}Mg_x$ alloys, using the methods of psuedopotential theory.[7,8] Since the properties of both Li and Mg are fairly well described by these methods (see, e.g., Refs. 7 and 9), the obtained estimates of the character of the singularities seem to be sufficiently reliable and are apparently a feature common of transitions of order $2\frac{1}{2}$ in both the concentration and the density.

In Sec. 2 we present the indicated general results on the singularities of $l$, $\rho$, and $\alpha$ near transitions of order $2\frac{1}{2}$. In Sec. 3 we derive formulas for the calculation of the resistance of a bcc metal in the two-wave approximation.[3,7,8] These formulas are used later to obtain quantitative estimates of $\rho$ and $\alpha$. They are also of independent interest and can be used for many bcc metals and alloys with FS close to (110) faces of the BZ. The answer is reduced to a form convenient for numerical calculations. In Sec. 4 are presented and discussed the results of such calculations for the $\rho(x)$ and $\alpha(x)$ dependences in $Li_{1-x}Mg_x$ alloys. These results show in particular that measurements of $\rho$ and $\alpha$ can serve as an effective method of both observing and determining a topological transition of order $2\frac{1}{2}$. The Conclusion discusses the possibility of using the considered effects for the investigation of the properties of FS in metals and alloys.

## 2. SINGULARITIES OF THE MEAN FREE PATH, CONDUCTIVITY, AND THERMOELECTRIC POWER IN PHASE TRANSITIONS OF ORDER 2½

We consider for simplicity region of low $T$, where the principal relaxation mechanism for the electrons is scattering by impurities [although accurate to $T/\mu$ and $\Theta_D/\mu$ ($\Theta_D$ is the Debye temperature) all the conclusions are valid also for scattering by phonons]. The kinetic coefficients are expressed here in terms of a certain mean free path l(p) satisfying the equation[10]

0038-5646/81/040830-05$02.40
© 1981 American Institute of Physics

$$\mathbf{l}(\mathbf{p})=\tau_{\mathbf{p}}\left[N_{im}\int W(\mathbf{p},\mathbf{p}')\mathbf{l}(\mathbf{p}')\delta(E_{\mathbf{p}}-E_{\mathbf{p}'})\frac{2d^3\mathbf{p}'}{(2\pi\hbar)^3}+\mathbf{v}_{\mathbf{p}}\right]. \tag{1}$$

Here $N_{im}$ is the impurity density; $W$ is the scattering probability; $E_{\mathbf{p}}$ and $\mathbf{v}_{\mathbf{p}}=\partial E_{\mathbf{p}}/\partial\mathbf{p}$ are the energy and velocity of an electron with momentum $\mathbf{p}$; $\tau_{\mathbf{p}}$ is the "departure" relaxation time:

$$\tau_{\mathbf{p}}^{-1}=N_{im}\int W(\mathbf{p},\mathbf{p}')\delta(E_{\mathbf{p}}-E_{\mathbf{p}'})\frac{2d^3\mathbf{p}'}{(2\pi\hbar)^3}. \tag{2}$$

At the points $\mathbf{p}'=\mathbf{p}_c$ of the BZ, where FS tangency or overflow takes place, the function $W(\mathbf{p},\mathbf{p}')$ is generally speaking finite and regular. Therefore expression (2) has at small $\eta=E_{\mathbf{p}}-\mu$ and $z$ the same singularity as the electronic density of states,[1] and according to (1) a similar singularity is possessed by $\mathbf{l}(\mathbf{p})$:

$$\mathbf{l}(\mathbf{p})=\mathbf{l}_0(\mathbf{p})+[\pm(\eta+z)]^{1/2}\theta[\pm(\eta+z)]\mathbf{l}_1(\mathbf{p}), \tag{3}$$

where $\mathbf{l}_0$ and $\mathbf{l}_1$ have singularities not stronger than $x\theta(x)$ as $x=\eta+z\to 0$. Since different kinetic coefficients, particularly the electric and thermal conductivities $\sigma$ and $\varkappa$, are equal to integrals of $\mathbf{l}(\mathbf{p})$ over the FS with different weighting functions,[11] all of them contain the $(\pm z)^{1/2}\theta(\pm z)$ singularity.

The electronic part $\alpha_e$ of the thermoelectric coefficient $\alpha$ is connected with the conductivity $\sigma=1/\rho$ by the relation[10]

$$\alpha_e=\frac{\pi^2T}{3e}\frac{\partial\ln\sigma(\eta)}{\partial\eta}\bigg|_{\eta=0}, \tag{4}$$

i.e., $\alpha_e\sim(\pm z)^{-1/2}\theta(\pm z)$ according to (3). Thus, the thermoelectric power increases rapidly as $z\to 0$, and this increase is limited only by the smearing of the transitions. This singularities are easiest to observe at low $T\lesssim(\Theta_D^3/\mu)^{1/2}$, inasmuch as at large $T$ the total $\alpha$ contains a large contribution $\alpha_{ph}$ due to dragging by phonons[10]; this contribution has, just as $\sigma$, a weaker dependence $\sim(\pm z)^{1/2}\theta(\pm z)$.

## 3. CALCULATION OF THE RESISTIVITY OF A BCC METAL IN THE TWO-WAVE APPROXIMATION

We derive a formula for $\rho$ of a bcc metal in the two-wave approximation, bearing in mind the description of metals with a FS close to the points $N$ of the BZ [i.e., to the points $\mathbf{g}_i/2$, where $\mathbf{g}_i$ are the reciprocal-lattice vectors of the star $(1,1,0)2\pi/a$, and $a$ is the lattice constant]. including cases of tangency and overflow near these points. For simplicity, we neglect the smearing of the FS.

We start with the known variational expression for $\rho$[11,3]

$$\rho=\frac{1}{J^2}\frac{\pi\Omega}{2\hbar}\sum_{s,s'}\iint d\mathbf{p}\,d\mathbf{p}'\delta(E_{\mathbf{p}s}-\mu)\delta(E_{\mathbf{p}'s'}-\mu)(\Phi_{\mathbf{p}s}-\Phi_{\mathbf{p}'s'})^2L_{\mathbf{p}s,\mathbf{p}'s'}, \tag{5a}$$

$$J=e\sum_{s}\int d\mathbf{p}\,v_{\mathbf{p}s}^{\parallel}\Phi_{\mathbf{p}s}\delta(E_{\mathbf{p}s}-\mu), \tag{5b}$$

with the customarily employed trial function $\Phi_{\mathbf{p}s}=\text{const.}\,v_{\mathbf{p}s}^{\parallel}$. Here $\Omega$ is the volume of the unit cell; $\mathbf{p}$, $s$, and $E_{\mathbf{p}s}$ are the momentum, band number, and energy of the electron; $v_{\mathbf{p}s}^{\parallel}$ is the component of the velocity $\mathbf{v}_{\mathbf{p}s}=\partial E_{\mathbf{p}s}/\partial\mathbf{p}$ along the electric field. For scattering of electrons by phonons, the quantity $L_{\mathbf{p}s,\mathbf{p}'s'}$ is of the form[11]

$$L_{\mathbf{p}s,\mathbf{p}'s'}^{ph}=\frac{\hbar^2}{4MT}\sum_{\nu=1}^{3}(M_{\mathbf{p}s,\mathbf{p}'s'}^{ph})^2/\mathrm{sh}^2\left(\frac{\hbar\omega_{\mathbf{q}\nu}}{2T}\right), \tag{6a}$$

and in the case of scattering by impurities (in an alloy)

$$L_{\mathbf{p}s,\mathbf{p}'s'}^{im}=x(1-x)(M_{\mathbf{p}s,\mathbf{p}'s'}^{im})^2. \tag{6b}$$

Here $M_{\mathbf{p}s,\mathbf{p}'s'}^{ph}$ and $M_{\mathbf{p}s,\mathbf{p}'s'}^{im}$ are the matrix elements for scattering by phonons and impurities, and will be discussed below; $\mathbf{q}=\mathbf{p}-\mathbf{p}'$, $\nu$, and $\omega_{q\nu}$ are the wave vector, polarization, and frequency of the phonon; $M$ is the ion mass. In the description of a disordered alloy $A_{1-x}B_x$ we shall use the approximation of an "average" (or "virtual") crystal,[6,7] and replace $M$ and $\Omega$ by their mean values:

$$M=(1-x)M_A+xM_B,\quad \Omega=a^3/2=(1-x)\Omega_A+x\Omega_B$$

[the latter is usually close to the experimental $\Omega(x)$, Ref. 12].

We break up the BZ of a bcc lattice into 12 equivalent sectors adjacent to the faces with centers $\mathbf{g}_i/2$ (see Fig. 1), and in each sector we use for the electron wave function $\psi_{\mathbf{p}s}$ the two-wave approximation[3]

$$\psi_{\mathbf{p}s}=\alpha_{\mathbf{p}s}e^{i\mathbf{p}\mathbf{r}}+\beta_{\mathbf{p}s}e^{i(\mathbf{p}-\mathbf{g}_i)\mathbf{r}}, \tag{7}$$

where $\alpha_{\mathbf{p}s}^2+\beta_{\mathbf{p}s}^2=1$. It is known that for $\mathbf{p}$ close to $\mathbf{p}_c=\mathbf{g}_i/2$ account must be taken of the second term of (7), corresponding to reflection from the opposite face of the BZ, whereas other reflections can be neglected in considered weak-pseudopotential approximation.[7,8]

We introduce in each sector a cylindrical coordinate system with center at $\mathbf{p}=0$ and with $z$ axis directed along $\mathbf{g}_i$ ($\Gamma N$ axis on Fig. 1), and change from $\mathbf{p}$ and $E_{\mathbf{p}s}$ to the dimensionless variables $\mathbf{p}/p_c=\mathbf{k}=(z,r,\varphi)$ and $\varepsilon_{\mathbf{k}s}=E_{\mathbf{p}s}/\varepsilon_c^0$, where

$$p_c=g/2,\quad \varepsilon_c^0=p_c^2/2m,$$
$$g=|\mathbf{g}_i|=2^{1/2}\pi/a,$$

and $m$ is the electron mass. The expressions for $\varepsilon_{\mathbf{k}s}$, $\alpha_{\mathbf{p}s}$, and $\beta_{\mathbf{p}s}$ in each sector then take the form

$$\varepsilon_{\mathbf{k}1,2}=1+r^2+(1-z)^2 \mp[u^2+4(1-z)^2]^{1/2}, \tag{8a}$$

$$\alpha_{\mathbf{p}1,2}=\left(\frac{1}{2}\pm\frac{1-z}{[u^2+4(1-z)^2]^{1/2}}\right)^{1/2}$$

$$\beta_{\mathbf{p}1,2}=\mp(1-\alpha_{\mathbf{p}1,2}^2)^{1/2}\,\mathrm{sgn}\,v(g). \tag{8b}$$

Here $v(g)=V(g)/\mathcal{E}(g)$ is the matrix element of the pseudopotential (which we assume for simplicity to be local), with account taken of the screening function

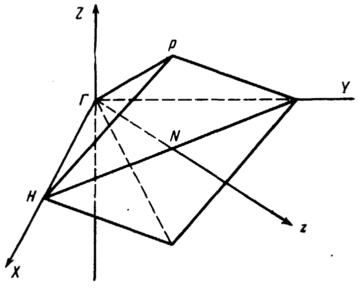

FIG. 1. One of the 12 equivalent sectors of the Brillouin zone of a bcc lattice.

$\mathcal{E}(g)$ (Refs. 7 and 13) and $u=|v(g)|/\varepsilon_c^0$. For an alloy we have in the average crystal approximation $v(g) = (1-x)v_A(g) + xv_B(g)$.

When integration is carried out in (5a) with respect to $\mathbf{p}'$ and $\mathbf{p}$ that lie in the sectors with vectors $\mathbf{g}_i$ and $\mathbf{g}_j$, there are only five nonequivalent relative orientations of $\mathbf{g}_i$ and $\mathbf{g}_j$. Thus, if $\boldsymbol{\nu}_i = 2^{1/2}\mathbf{g}_i/g$ is equal to $\boldsymbol{\nu}_1=(1,1,0)$, the $\boldsymbol{\nu}_j$ of these nonequivalent sectors can be chosen to be $\boldsymbol{\nu}_1=(1, 1, 0)$, $\boldsymbol{\nu}_2=(1, 0, 1)$, $\boldsymbol{\nu}_3=(1, -1, 0)$, $\boldsymbol{\nu}_4=(0,-1,-1)$, and $\boldsymbol{\nu}_5=(-1,-1,0)$. The contributions made to (5a) by the integration over the equivalent sectors can then be multiplied by their numbers $N_j$: $N_1 = N_5 = 1$, $N_2 = N_4 = 4$, and $N_3 = 2$.

Bearing the foregoing remarks in mind, and integrating in (5a) with respect to the variables $r$ and $r'$ and in (5b) with respect to $r$ and $z$, we arrive at the following calculation formulas for $\rho$:

$$\rho=CR/J^2, \tag{9a}$$

$$R=\sum_{j=1}^{5}N_j\sum_{s,s'=1}^{2}\iint_0^{2\pi}\frac{d\varphi\,d\varphi'}{(2\pi)^2}\int_{z_s^l(\varphi)}^{z_s^u}dz\int_{z_{s'}^l(\varphi')}^{z_{s'}^u}dz'\,(\mathbf{v}_{\mathbf{k}s}-\mathbf{v}_{\mathbf{k}'s'})^2L^j_{\mathbf{k}s,\mathbf{k}'s'}, \tag{9b}$$

$$J=\int_0^{2\pi}\frac{d\varphi}{2\pi}[J_1(y_l)-J_2(y_u)]. \tag{9c}$$

The superscript $j$ of $L^j_{\mathbf{k}s,\mathbf{k}'s'}$ means that the vectors $\mathbf{k}$ and $\mathbf{k}'$ lie in the sectors with $\nu_j$ and $\nu_1$ indicated above $\boldsymbol{\nu}_{\mathbf{k}s}=\frac{1}{2}\partial\mathcal{E}_{ks}/\partial\mathbf{k}$, and the following notation was introduced:

$$C_{ph}=\hbar\pi^5/16e^2a(\varepsilon_c^0)^2,\qquad C_{im}=\hbar\pi^3a/32e^2(\varepsilon_c^0)^2, \tag{10a}$$

$$J_1(y)=(1+\tilde\mu)y-\frac{u}{2}\operatorname{arctg}\frac{2y}{u}+\frac{u^2}{2}\ln\left[y+\left(y^2+\frac{u^2}{4}\right)^{1/2}\right], \tag{10b}$$

$$J_2(y)=\theta_-J_1(-y)+\theta_+J_1(y),\qquad \theta_\pm=\theta(\pm\tilde\mu-u), \tag{10c}$$

$$\tilde\mu=(\mu-\varepsilon_c^0)/\varepsilon_c^0,\quad y_l=1-z_1^l(\varphi),\quad y_u=1-z_1^u. \tag{10d}$$

We note that in the employed model the point $\tilde\mu=-u$ corresponds to tangency, and $\tilde\mu=u$ corresponds to overflow of the FS at the point $N$. Therefore $\theta^-$ in (10c) corresponds to the region ahead of the tangency, and $\theta_+$ to the region past the overflow. The quantities $z_s^u$ and $z_s^l$ in (9) and (10) denote the limits of integration with respect to $z$. The upper limit $z_s^u$ is determined from the equation $E_{\mathbf{p}s}=\mu$ at $r=0$:

$$z_{1,2}^u=[1\mp(2+\tilde\mu-2(1+\tilde\mu+u^2/4)^{1/2})^{1/2}]\theta(|\tilde\mu|-u)+\theta(u-|\tilde\mu|). \tag{11}$$

The lower limit $z_2^l=1$, and $z_1^l$ is obtained from the condition that the surface $E_{\mathbf{p}s}=\mu$ intersect the lateral faces of the sectors (of the type $\Gamma PH$ in Fig. 1). This yields for $z_1^l=z_1^l(\varphi)$ the equation

$$(z_1^l)^2f(\varphi)+(1-z_1^l)^2-\tilde\mu=[u^2+4(1-z_1^l)^2]^{1/2},\qquad z_2^l=1, \tag{12}$$

where

$$f(\varphi)=(|\cos\varphi|+2^{1/2}|\sin\varphi|)^{-2}.$$

The matrix element of the phonon scattering in (6a) for the plane waves $\mathbf{p}$ and $\mathbf{p}'$ is of the form $M^{ph}_{\mathbf{pp}'} = (\mathbf{q}\cdot\mathbf{e}_{q\nu})v(\mathbf{q})$, where $\mathbf{q}=\mathbf{p}-\mathbf{p}'$ and $\mathbf{e}_{q\nu}$ is the phonon polarization vector.[7] For impurity scattering of plane waves we have in the employed approximations[11,7] $M^{im}_{\mathbf{pp}'}=v_A(\mathbf{q})-v_B(\mathbf{q})$. Therefore, taking into account the mixing of the states (7), we can express the matrix elements in (9) and (6) can be expressed in the form

$$M^j_{\mathbf{k}s,\mathbf{k}'s'}=\alpha_{\mathbf{k}s}\alpha_{\mathbf{k}'s'}\xi_{\mathbf{q},\nu}W(\mathbf{q})+\alpha_{\mathbf{k}s}\beta_{\mathbf{k}'s'}\xi_{\mathbf{q}+\mathbf{g}_1,\nu}W(\mathbf{q}+\mathbf{g}_1)$$
$$+\beta_{\mathbf{k}s}\alpha_{\mathbf{k}'s'}\xi_{\mathbf{q}-\mathbf{g}_j,\nu}W(\mathbf{q}-\mathbf{g}_j)+\beta_{\mathbf{k}s}\beta_{\mathbf{k}'s'}\xi_{\mathbf{q}+\mathbf{g}_1-\mathbf{g}_j,\nu}W(\mathbf{q}+\mathbf{g}_1-\mathbf{g}_j), \tag{13}$$

where we have for the phonon and impurity scattering in the alloy, respectively,

$$\xi_{\mathbf{q}\nu}^{ph}=\mathbf{q}\mathbf{e}_{\mathbf{q}\nu},\qquad W^{ph}(\mathbf{q})=v(\mathbf{q})=(1-x)v_A(\mathbf{q})+xv_B(\mathbf{q}), \tag{14a}$$

$$\xi_{\mathbf{q}\nu}^{im}=1,\qquad W^{im}(\mathbf{q})=v_A(\mathbf{q})-v_B(\mathbf{q}). \tag{14b}$$

To calculate the vectors $\mathbf{q}=\mathbf{k}-\mathbf{k}'$ and $\mathbf{v}_{\mathbf{k}s}-\mathbf{v}_{\mathbf{k}'s'}$ in (9) we must also change over to a single coordinate frame for all sectors. We choose it to be the system $XYZ$ connected with the first sector $j=1$ and indicated in Fig. 1. Then a transformation of the components of the vector $\mathbf{k}$ from the cylindrical frame $(z, r, \varphi)$ connected with the sector $j$ into this system for the components $k_x$, $k_y$, $k_z$ at $j=1, 2, 3, 4, 5$ yields respectively

$$(a, b, c),\quad (b, c, a),\quad (b, -a, c),\quad (c, -a, -b),\quad (-a, -b, c), \tag{15}$$

where

$$a=2^{-1/2}(z+r\cos\varphi);\quad b=2^{-1/2}(z-r\cos\varphi),\quad c=r\sin\varphi. \tag{16}$$

Analogously, the velocity components $\mathbf{v}_{\mathbf{k}s}$ for each of the sectors are determined by formulas (15) with $a$, $b$, and $c$ replaced by the values $a_s$, $b_s$, and $c_s$, which are connected with $a$, $b$, and $c$ of (16) as follows:

$$a_{1,2}=a-\frac{1}{2^{1/2}}\pm\frac{2^{1/2}d}{(u^2+4d^2)^{1/2}},\quad b_{1,2}=b-\frac{1}{2^{1/2}}\pm\frac{2^{1/2}d}{(u^2+4d^2)^{1/2}},$$
$$c_{1,2}=c,\qquad d=1-2^{-1/2}(a+b). \tag{17}$$

Finally, when calculating $\rho(x)$ of an $A_{1-x}B_x$ alloy with valences $z_A$ and $z_B$, the dependence of the chemical potential $\mu$ on $x$ is determined from an equation that connects the volume bounded by the FS with the average number of electrons per atom, $\bar z=(1-x)z_A+xz_B$:

$$\frac{\bar z}{3\pi\sqrt2}=\int_0^{2\pi}\frac{d\varphi}{2\pi}\left[\frac13(z_1^l)^2f(\varphi)+I_1(y_l)\right]+I_2(y_u), \tag{18}$$

where

$$I_1(y)=\tilde\mu y-\frac{y^3}{3}+y\left(y^2+\frac{u^2}{4}\right)^{1/2}+\frac{u^2}{4}\ln\left[\frac{2y}{u}+\left(1+\frac{4y^2}{u^2}\right)^{1/2}\right], \tag{19}$$
$$I_2(y)=\theta_+I_1(y)+\theta_-I_1(-y)$$

and $\theta_\pm$, $z_1^l$, $y_l$, $y_u$, and $f(\varphi)$ are the same as in (10) and (12).

## 4. CALCULATION RESULTS FOR Li-Mg ALLOYS

For the alloys $\mathrm{Li}_{1-x}\mathrm{Mg}_x$, the total pseudopotential $V_{\mathrm{Li}}(\mathbf{q})$ in (14) was taken from Ref. 9, and $V_{\mathrm{Mg}}(\mathbf{q})$ was obtained by the same method as in Ref. 9, using the Geldart-Vosko approximation of the screening function $\mathcal{E}(\mathbf{q})$.[13,14] These pseudopotentials were used also in the calculations of the frequencies and polarizations of the phonons in (6a) and (14a), thereby ensuring apparently a sufficient accuracy of these quantities.[7,9] For the components $v(g)$ (or $u$) in (8)–(12) and (17)–(19), however, which determine in the employed model all the phenomena connected with the $2\frac12$-order transition, it is desirable to use the most realistic values available. At the same time, the simple local-pseudopotential approximation may be quite inaccurate here, especially for Li.[7] We therefore used for the quantities $u_i$

$= |v_i(g)|/\varepsilon_c^0$ (where $i$ stands for Li or Mg), values obtained by fitting $v_i(g)$ to the data on the FS of these metals,[7] namely $u_{\rm Li} = 0.18$ and $u_{\rm Mg} = 0.09$ (set $a$). To investigate the sensitivity of the results to the values of $u_i$, we used also values half as large, $u_{\rm Li} = 0.09$ and $u_{\rm Mg} = 0.045$ (set $b$).

The tangency of the FS to the point $N$ of the BZ, defined by the relation $\tilde{\mu}(x) = -u$ with $\tilde{\mu}(x)$ taken from (18), takes place for set $a$ at a concentration $x_c = x_c^a = 0.247$ and for set $b$ at $x_c^b = 0.353$ (in the free electron model, $x_c = x_c^0 = 0.48$). The overflow regions $\tilde{\mu}(x) \geqslant u$, on the other hand correspond to large $x \geqslant x_{c2} \sim 0.7$ ($x_{c2}^a = 0.75$ and $x_{c2}^b = 0.65$), whereas at $x = 0.70$ the alloy $\mathrm{Li}_{1-x}\mathrm{Mg}_x$ already loses in fact its bcc structure.[12] In addition, calculations at $x > x_{c2}$ are made somewhat more elaborate by the addition of the $s \to s'$ interband transitions with $(s, s') = (1, 2)$, $(2, 1)$, and $(2, 2)$. The calculations were performed therefore only for $x < x_{c2}$, while for the region $x < x_{c2}$ we confined ourselves to a qualitative discussion.

The calculation results are shown in Figs. 2 and 3. To decrease the influence of the inaccuracies connected with the choice of the pseudopotential and of other approximations of the model, we present the results for the relative quantities $\rho^*_{ph}(x) = \rho_{ph}(x)/\rho_{ph}(0)$ in the case of phonon scattering and $\rho^*_{im}(x) = \rho_{im}(x)/\tilde{\rho}_{im}(0)$, where $\tilde{\rho}_{im}(x) = \rho_{im}(x)/x(1-x)$ in the case of impurity scattering. In the coefficient $\alpha_e(x)$, on the other hand, the inessential factors drop out in accord with the definition (4). For impurity scattering (6b) and (14b) the results shown in Fig. 2 are for values of $u_i$ from both sets $a$ and $b$; for phonon scattering (6a) and (14a), the results of Fig. 3 are for $T = 80\ K$ and for $u_i$ from set $a$.

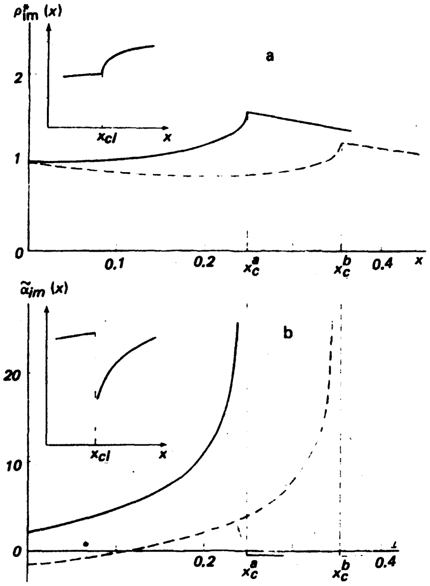

FIG. 2. $a$) Plot of relative reduced resistivity $\rho^*_{im}(x) = \tilde{\rho}_{im}(x)/\tilde{\rho}_{im}(0)$, where $\tilde{\rho}_{im}(x) = \rho_{im}(x)/x(1-x)$ for impurity scattering in an $\mathrm{Li}_{1-x}\mathrm{Mg}_x$ alloy in the model of Sec. 3. The inset indicates the qualitative behavior of $\rho^*(x)$ near the overflow point $x_{c2}$. $b$) Plot of reduced thermoelectric power coefficient $\alpha_{im}(x) = \alpha_e^{im}(x)/\alpha_0$, where $\alpha_0 = \pi^2 T/3\,|e|\,\varepsilon_c^0$ and $\alpha_e^{im}$ is given by Eq. (4) with $\sigma = 1/\rho_{im}$. The inset shows the qualitative form of $\tilde{\alpha}_{im}(x)$ near $x = x_{c2}$. The solid curves correspond to the values of $u_{Li}$ and $u_{\rm Mg}$ from set $a$, and the dashed ones, from set $b$, see the text.

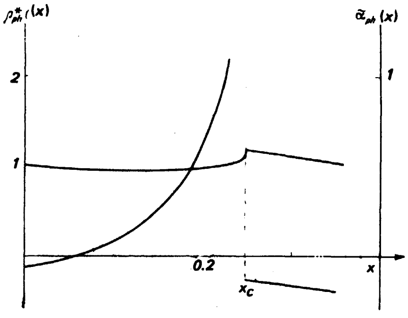

FIG. 3. Plot of $\rho^*_{ph}(x) = \rho_{ph}(x)/\rho_{ph}(0)$ and of $\tilde{\alpha}_{ph}(x) = \alpha_e^{ph}(x)/\alpha_0$ for the phonon mechanism of scattering in the alloy $\mathrm{Li}_{1-x}\mathrm{Mg}_x$ at $T = 80$ K and $u_{\rm Li}$ and $u_{\rm Mg}$ from set $a$. Solid curve—$\rho^*_{ph}(x)$, curve with break—$\tilde{\alpha}^*_{ph}(x)$.

It is seen from Fig. 2a that as the transition point $x_c$ is approached the impurity resistivity increases rapidly, by approximately 1.5 times, whereas at $x > x_c$ it varies weakly and linearly with $x$. The anomaly of the coefficient $\alpha_e(x)$ in Fig. 2b is correspondingly very abrupt. For both sets of parameters $u_i$, the variation of $\rho(x)$ near $x_c$ is described with good accuracy by the formula

$$\tilde{\rho}(x) = \tilde{\rho}(x_c)\left[1 - A\left(\frac{\mu_c - \mu}{\varepsilon_c^0}\right)^{1/2}\theta(\mu_c - \mu) - B\frac{\mu - \mu_c}{\varepsilon_c^0}\theta(\mu - \mu_c)\right], \quad (20)$$

where $\mu_c = \mu(x_c)$, $A^a = 1.75$, $B^a = 3.2$ and $A^b = 1.9$, $B^b = 2.7$. The magnitude of the anomalies is thus not very sensitive to the parameters of the model.

It is seen from Fig. 2 that the singularities of $\rho$ and $\alpha$ appear in the concentration interval $\Delta x \sim 3$–$5\%$, which corresponds to the interval $\Delta z = \mu - \mu_c = 0.1$–$0.15$ eV. Allowance for the concentration smearing $\Delta\varepsilon_x$ of the FS in the alloy leads to a certain smearing of these singularities. They will, however, be sufficiently pronounced if $\Delta z \gtrsim \Delta\varepsilon_x$ (the temperature spread is $\Delta\varepsilon_T \sim T \ll \Delta z$). Estimates of $\Delta\varepsilon_x$ by the coherent-potential method[6] yield $\Delta\varepsilon_x \sim 0.06$–$0.08$ eV for CuZn alloys and $\Delta\varepsilon_x \sim 0.1$–$0.15$ for CuNi; if these estimates are used, then $\Delta z \gtrsim \Delta\varepsilon_x$. The described anomalies of $\rho$ and $\alpha$ in alloys are thus apparently fully observable, and the degree of their smearing can yield information on the values of $\Delta\varepsilon_x$.

In scattering by phonons (Fig. 3), the singularities pf $\rho$ are smaller than for scattering by impurities: $\Delta\rho^*_{ph} \sim 20\%$. The singularity of the coefficient $\alpha_e$ is clearly pronounced, as before, but the absolute values of $\alpha_e^{ph}$ are smaller by one order than those of the impurity $\alpha_e^{im}$. $\rho^{im}$ also predominates in the total resistivity $\rho \approx \rho^{im} + \rho^{ph}$ of the alloy at $x$ that are not small and at $T$ that are not too high. The results shown in Fig. 3 for the alloys in question are thus more readily methodological. All the results of Figs. 2 and 3, however, seem to illustrate the general character of the anomalies of $\rho$ and $\alpha$ for transitions of order $2\frac{1}{2}$, with respect to both concentration and pressure. Figure 3 can therefore describe the anomalies of $\rho$ and $\alpha$ for transitions in pure metals, say under pressure, and indicate in particular that in transitions of order $2\frac{1}{2}$ these anomalies are noticeably smaller for the phonon scattering mechanism than for the impurity mechanism.

The insets in Figs. 2a and 2b illustrate the character of the anomalies in the case of overflow of the FS through a Brillouin zone face. It is seen, in particular, that $\alpha_e$ has now a strongly asymmetrical minimum in place of a maximum. The forms of the anomalies of $\rho$ and $\alpha$ make it therefore possible to determine also the character of the variation of the FS topology in the transition.

Finally, a note concerning the possible connection between the effects discussed and the peculiar dependence of $\rho$ on the pressure $P$ observed in Li.[15] When $P$ increases from 0 to $P_{cr} \sim 70$ kbar, the value of $\rho$ in Li, in contrast to other alkali metals, does not decrease but increases by approximately 30%. The FS of Li is noticeably elongated towards the (110) faces of the BZ,[16] and upon compression this elongation seems to increase (just as in the calculations of Ref. 17 for Cs). Therefore, with increasing $P$, the FS can rapidly approach the point $N$ of the BZ, and then the growth of $\rho(P)$ can have the same appearance as in Figs. 2 and 3. To be sure, the abrupt decrease of $\rho$ at $P = P_{cr}$, observed in Ref. 15, is not explained by the described picture of the transition of order $2\frac{1}{2}$, but it is apparently connected with some sort of first-order transition, to which a proximity of the FS to BZ faces can contribute.[7]

## 5. CONCLUSION

We note once more that according to the presented discussion the anomalies of $\rho$ and $\alpha$ can serve as an effective tool for the identification of transitions of order $2\frac{1}{2}$. This is topical, in particular, because hypotheses postulating the presence of such transitions are being recently invoked to explain other observed phenomena. Thus, for example, in Ref. 18 these hypotheses are used in a discussion of the anomalies in the dependences of the superconducting-transition temperatures of Mo–Re alloys on concentration and pressure. As seen from the foregoing, these hypotheses can be quite simply verified experimentally by measuring $\rho$ and $\alpha$ (in the normal state).

Another important application of the considered effects may be their use to investigate the degree $\Delta\varepsilon_x$ of the spreading of the FS of alloys. These questions are attracting great interest,[6] particularly in connection with known with the Hume-Rothery opinions concerning the connection between the FS and BZ in alloy theory.[7] At the same time, experimental information on $\Delta\varepsilon_x$, as already noted, is extremely limited. According to the foregoing remarks, an investigation of the form of the anomalies of $\rho$ and particularly of $\alpha$ in the region of a transition of order $2\frac{1}{2}$ can serve as the source of quantitative information on the spreading of the FS, and hence on the applicability of the quasimomentum concept to the description of electronic states in alloys.

The authors thank M. I. Kaganov and I. M. Lifshitz for a discussion of the work.

[1] I. M. Lifshitz, Zh. Eksp. Teor. Fiz. 38, 1569 (1960) [Sov. Phys. JETP **11**, 1130 (1960)].

[2] M. I. Kaganov and I. M. Lifshitz, Usp. Fiz. Nauk 129, 487 (1979) [Sov. Phys. Usp. 22, 904 (1979)].

[3] J. M. Ziman, Proc. Roy. Soc. A252, 63 (1959).

[4] I. M. Lifshitz, M. Ya. Azbel', and M. I. Kaganov, Elektronnaya teoriya metallov (Electron Theory of Metals), Nauka, 1971, §13 [Consultants Bureau, 1973].

[5] B. N. Powell, P. Martel, and A. D. B. Woods, Phys. Rev. **171**, 727 (1968). S. C. Ng and B. N. Brockhouse, Neutron Inelastic Scattering, IAEA, Vienna, 1, 253 (1968).

[6] H. Eherenreich and L. Schwarz, Electron Structure of Metals [Russ. transl.], Mir, 1979.

[7] V. Heine, M. Cohen, and D. Ware, Pseudopotential Theory [Russ. transl.], Mir, 1973.

[8] W. A. Harrison, Pseudopotentials in the Theory of Metals, Benjamin, 1966.

[9] V. G. Vaks and A. V. Trefilov, Fiz. Tverd. Tela (Leningrad) 19, 244 (1977) [Sov. Phys. Solid State **19**, 139 (1977)].

[10] E. M. Lifshitz and L. P. Pitaevskiĭ, Fizicheskaya kinetika (Physical Kinetics), Nauka, 1979.

[11] J. M. Ziman, Electrons and Phonons, Oxford, 1960.

[12] M. Hansen and K. Anderko, Constitution of Binary Alloys, McGraw, 1958.

[13] R. W. Shaw, J. Phys. C 3, 1140 (1970).

[14] D. J. W. Geldart and S. H. Vosko, Canad. J. Phys. **44**, 2137 (1966).

[15] R. A. Stager and H. G. Drickamer, Phys. Rev. 132, 124 (1963).

[16] M. J. G. Lee, Phys. Rev. 178, 953 (1969).

[17] J. Yamashita and S. Asano, J. Phys. Soc. Jpn 29, 264 (1970). S. Louie and M. L. Cohen, Phys. Rev. B10, 3237 (1974).

[18] T. A. Ignat'eva and Yu. A. Cherevan', Pis'ma Zh. Eksp. Teor. Fiz. 31, 389 (1980) [JETP Lett. 31, 361 (1980)].

Translated by J. G. Adashko